The Parkes Front-End Controller and Noise-Adding Radiometer

T. J. Brunzie
Radio Frequency and Microwave Subsystems Section

A new front-end controller (FEC) was installed on the 64-m antenna in Parkes, Australia, to support the 1989 Voyager 2 Neptune encounter. The FEC was added to automate operation of the front-end microwave hardware as part of the Deep Space Network's Parkes–Canberra Telemetry Array. Much of the front-end hardware was refurbished and reimplemented from a front-end system installed in 1985 by the European Space Agency for the Uranus encounter; however, the FEC and its associated noise-adding radiometer (NAR) were new JPL designs. Project requirements and other factors led to the development of capabilities not found in standard DSN controllers and radiometers. The Parkes FEC/NAR performed satisfactorily throughout the Neptune encounter and was removed in October 1989.

I. Introduction

The 64-meter Parkes Antenna of the Australian Telescope National Facility (or the Parkes antenna) was temporarily used to enhance X-band (8.42 GHz) receiving capability from the Voyager spacecraft during the Neptune encounter in 1989. The Parkes antenna formed part of the DSN Parkes–Canberra Telemetry Array (PCTA) and was outfitted with DSN-compatible hardware, including a microwave front end, telemetry receiver, data recorders, and radio science equipment. Much of the hardware was refurbished and reimplemented from the front-end system developed by the European Space Agency (ESA) for the Uranus encounter in 1986; however, the previous front-end monitor and control system was replaced with a new JPL design. (For an overall description of the design and installation of the front-end system, see [1,2].) A block diagram of the front-end system is shown in Fig. 1.

The Parkes front-end controller (FEC) centralized and automated the monitoring and control of the front-end system, tying together equipment located in a NASA trailer next to the antenna with hardware located in the antenna's aerial cabin. A block diagram of the FEC is shown in Fig. 2.

The primary tasks performed by the FEC were to

(1) Monitor and control the antenna waveguide switches and the polarizer drive assembly using a remote switch/control unit and telltale monitoring.

(2) Measure system operating noise temperatures using the Y-factor technique through the automated waveguide switches, quartz thermometer, dual traveling-wave maser (TWM) control assembly, and power meter.

(3) Measure gain versus frequency of the TWMs, with storage, retrieval, and display.

(4) Perform remote-controlled, noise-adding radiometer functions through automation of the noise diodes and the RF detector power meter during antenna calibration. Functions included returning a time-varying analog signal, representing operating noise temperature, and periodic calibration of the noise diodes.

(5) Chart performance history, provide status updates, and generate alarm messages for the closed-cycle refrigerator/compressor monitor system [3].

(6) Monitor alarms for the downconverters, monitor receiver, and test signal upconverter, including power supplies, local oscillator power levels, timing, and phase-lock conditions.

The overall functions and components of the Parkes FEC are described in [1], which details the front-end system design before it was implemented. This article will focus primarily on the noise-adding radiometer (NAR) function of the FEC, since adding this capability comprised a major design effort during FEC development.

Typically, NARs at DSN tracking stations are implemented in the form of a precision power monitor (PPM) assembly [4]. But in the case of the Parkes antenna, a PPM was not installed for the Neptune encounter because of budgetary constraints. Instead, a new NAR design was developed as part of the new Parkes front-end controller.

The NAR met all requirements (see Table 1) and functioned without difficulty during the Voyager Neptune encounter. The FEC/NAR equipment was removed from the Parkes antenna on October 2, 1989 and returned to JPL.

II. NAR Requirements

As was mentioned, one of the functions performed by the Parkes FEC was radiometric measurement of the operating noise temperature of the receiving systems. System noise temperature data are needed for RF feed focusing, collection of pointing data, and measurement of baseline atmospheric effects. All radiometers determine noise temperature by comparing receiver noise level against a calibrated noise source. The radiometer most commonly used in the DSN is referred to as a noise-adding radiometer because it periodically adds calibrated noise to the signal during the measurement process [5].

Requirements for the Parkes NAR originated from the need to calibrate the pointing and focus of the antenna after the new front-end package was installed. This type of calibration is performed by pointing the antenna at extragalactic radio sources, quasi-stellar objects that radiate at radio frequencies. The resulting increase in receiver noise level caused by these radio sources appears as a rise in noise temperature that is detected and measured by the radiometer. Optimum antenna focus and pointing calibration is achieved by varying equipment positions and other parameters in the aerial cabin, RF package, and feedhorn until a peak in system noise temperature is obtained.

During pointing calibration, the telescope makes two orthogonal sweeps across the catalog coordinates of a star, digitizing and recording the system temperature as a function of position. The antenna system computer derives a Gaussian curve from each sweep, then mathematically constructs a model that fits these Gaussian curves to previously cataloged information on the flux and position of the star. The difference between the cataloged values and the center of the sweep is the pointing error. The procedure is repeated for several combinations of azimuth and elevation angles to model and systematically eliminate these pointing errors. However, these pointing curves are distorted somewhat by poor gain stability in the receiving system and also by insufficient NAR sample resolution. The stability requirement for the Parkes NAR was 0.1 K during the sampling time (corresponding to a gain stability of 0.02 dB) and the resolution requirement was 0.01 K for returned samples.

Ideally, the computers that control the pointing and focusing of the Parkes antenna would receive a continuous, instantaneous feedback of system temperature with infinite resolution. In practice, each measurement is limited in resolution and requires some minimum amount of integration time before a suitable system temperature sample can be produced. The Parkes NAR was required to return samples at a rate of 10 per second or faster, with 20 samples per second desired. These temperature samples were to be supplied as time-varying analog voltages sent to the control room through coaxial cable.

Other constraints limited design options for the Parkes NAR. Since radiometer sample resolution, sampling rate, system temperature, noise-diode selection, and system hardware characteristics are not independent parameters, they could not be designed as such. Attempts were made

to minimize conflicts in requirements through efficient software design, but some trade-off in performance was necessary. Project requirements that limited the design included the need to use existing PPM components to save time and reduce cost and the need to time-share hardware and software with other front-end functions.

III. FEC/NAR System Description

The Parkes tracking station (designated DSS 49) was configured for the Voyager Neptune encounter as a two-channel X-band receive-only system, using two cryogenic maser amplifiers. The front-end package, which contained both masers and the microwave feed, was positioned at the prime feed focus in the antenna's aerial cabin. The NAR noise-diode assemblies and support equipment were part of the front-end package. The Voyager telemetry receiver and associated signal-processing equipment were located in a double-wide trailer just outside the antenna pedestal. The associated FEC equipment was divided between these two locations (see Fig. 1) [2].

A. Front-End Controller

1. Description. The FEC consisted of a multibus computer providing a card cage, power supply, and enclosure with slides. It monitored and controlled the microwave electronics in the antenna front end and provided for two modes of radiometer operation: total-power and noise-adding. A block diagram of the FEC is shown in Fig. 2.

The FEC central processing unit (CPU) was a Multibus-based Intel 8086 single-board computer containing GP-IB and digital-to-analog (D/A) converter piggyback cards. FEC support boards included two ROM boards, a RAM board, a four-port serial communications board, a 3- by 24-bit parallel communications board, and a JPL-built pulse-train frequency counter board. Most of the hardware interfaces for NAR operation used ports on input/output (I/O) boards shared with other FEC functions. The only additional hardware added to the FEC for NAR operation was the D/A converter card and the pulse-train frequency counter board. Monitor and control signals for the NAR shared the same communications network used by other FEC functions.

The FEC D/A converter provided two analog signals for NAR operation, the control signal for the RF power-detector drawer (RF detector) internal attenuator and the analog system temperature output. A channel on the parallel I/O board provided 16 bits for the RF detector input channel select and confirmation telltales as well as the diode modulation drive output. Noise diode selection and confirmation was performed via an IEEE-488 GP-IB interface to an HP 3488A switch/control unit located in the aerial cabin.

The pulse-train frequency counter board, a standard PPM design, provided an integrate-and-dump means of measuring the output frequency of the RF detector drawer (which is a function of input power). Once instructed to begin a measurement, the board operated unattended, interrupting the CPU when data collection was completed. By counting input pulses and system clock ticks simultaneously, the board allowed the FEC to collect both timing and RF power data. Dividing the number of input pulses by measurement duration yielded average frequency, which was then further processed to yield input power and system temperature, as will be discussed further in Section B.

2. Operation. The FEC was controlled through three CRT terminals, each able to issue commands and receive displays. The "local" terminal was located in one of the front-end control racks in the trailer and was used for front-end maintenance and testing. It also was used exclusively for operation of the NAR during spacecraft tracking. The "remote" terminal was located in the antenna control room on the third floor of the antenna pedestal and was used by Parkes personnel to operate the NAR in support of antenna calibration and X-band radio astronomy observations. The "data link" terminal was located in the control room at the Canberra Deep Space Communications Center (CDSCC) and was used to monitor front-end health and status via modem during pre-encounter periods when the antenna was not being operated by station personnel.

All three of these terminals were able to send commands and monitor front-end status at any time, but only one terminal at a time functioned as the master terminal, possessing the ability to lock the front-end configuration for security during actual tracking operations. The master terminal was selected via a switch on the front of the FEC chassis. All data, commands, and information graphics could be printed on a local printer.

Radiometer data were made available by CRT displays, printouts, and via a time-varying analog signal. The display information (which could be suppressed to prevent interference with other FEC commands) was copied to all three terminals for simultaneous display. Printouts of these displays were made by connecting a printer to the CRT. The analog output, available at the FEC back panel, represented system temperature values as voltage levels. This signal was updated with each temperature sample computed, transmitted to the pedestal third floor

via coaxial cable, and used to drive a strip-chart recorder and analog front end on the Parkes antenna computer for pointing calibration and radio science data collection.

3. Commands. Commands for the FEC were grouped into menus according to function. Each menu item included the command name, a brief functional description, and a syntactic representation of parameter types. Syntax and range checking was enforced; individual error messages explained how to correct command errors. Each group had a menu and one or more corresponding status displays. Most commands also responded to a "query," which produced a one-line status display for the associated function. FEC menus and status displays that pertained to the radiometer are shown in Figs. 4 through 9.

4. Interfaces. The FEC provided cabling interfaces with the front-end equipment via IEEE 488, parallel-transistor-transistor logic (TTL) control lines, RS-232 serial communication lines, and 50-ohm coax. The equipment interfaces are described in [1].

B. Noise-Adding Radiometer

It is difficult to describe the NAR on a component level; it can more readily be conceptualized as a function of the FEC than as a set of components. Dedicated NAR components included the noise diode assemblies (located on the maser package in the aerial cabin), RF power-detector drawer (located below the FEC in front-end control cabinet no. 2), and its associated frequency-counter board (located within the FEC). These components are described below, along with NAR operation and calibration. A description of the NAR design before it was implemented is detailed in [6]; however, several changes have been made to this design since the report was published. Block diagrams of the NAR are shown in Figs. 2 and 3.

1. Noise-Diode Assemblies. Two noise-diode assemblies were recovered from the ESA Parkes front-end system, implemented during the Voyager Uranus encounter in 1986. Each assembly consisted of an oven with three diodes and a power supply. Each diode was capable of three noise levels, depending on the value of its supply current. The diode's power supply assembly contained three independent current sources, one per diode. Any of the three current levels could be selected through three relay inputs and monitored with three relay telltales. A separate TTL-level input for each diode provided instant switching of the supply current, allowing rapid diode modulation.

The relay inputs, telltales, and modulation-drive signals were designed to be monitored and controlled by a PPM through a PPM NAR controller assembly. But, in this case, the PPM controller was functionally replaced by the FEC, which controlled the noise diodes with an HP 3488A switch/control unit (SCU). This unit was a rack-mounted programmable device that used removable interface cards to monitor and control various functions. Communication with the SCU was provided by an IEEE-488 GP-IB standard bus that connected the FEC with equipment in the trailer and the aerial cabin.

Two SCU bidirectional digital I/O interface cards were used by the NAR to drive the noise diode power supply relays and to sense the relay tell-tales. Each card provided sixteen channels programmed for eight bits input and eight bits output. Although there are potentially nine inputs and nine outputs for each noise diode assembly, only seven diode temperatures were standard on the units: 0.25, 0.5, 1, 2, 4, 8, and 50 K. Each card provided independent closed-loop diode selection for one of the two maser channels.

Because diode modulation requires precisely coordinated switching that the SCU cannot provide when using a remote, shared GP-IB, the SCU was not used for this purpose. A single modulation signal was transmitted separately from the trailer on a coaxial cable and used to modulate all six diodes simultaneously. And because the project requirements for the NAR were limited to pretrack calibration support, no attempts were made to provide the multiple-diode selection and independent modulation schemes sometimes desired for radio science applications.

Noise output was injected through a waveguide coupler between the feedhorn/ambient load switches and the maser input flanges. The maser input flange served as the reference point for calculating system temperatures. The actual power measurements were made at the PCTA telemetry receiver input in the equipment trailer.

2. RF Power-Detector Assembly. The Parkes NAR RF power-detector assembly was a borrowed PPM 8.4-GHz (X-band) prototype square-law detector [7]. Originally, as described in [6], plans were made to use digital signal-processing techniques to develop an alternative to the PPM detector (the digital power meter). This choice was motivated by the poor linearity of the PPM device, which results in inaccurate measurements. Because of budgetary constraints, however, the RF power detector was incorporated into the Parkes radiometer design instead.

In typical DSN use, the RF detector is part of a PPM operated by a PPM NAR controller [4]. However, for the Parkes implementation, the detector was operated by

the FEC. The name "square-law" refers to the square-law diode used by the detector to measure input signal power: the voltage developed across the diode is proportional (ideally) to the total power in the signal. This voltage is translated into a TTL-level pulse train whose frequency represents signal power; the pulse train forms the output of the assembly. For the 1989 Voyager encounter, the pulse-train frequency was measured using a JPL-designed digital frequency-counter board.

Although the input power–output frequency relationship of the RF detector assemblies was intended to be linear, in practice it more closely resembled a parabola than a straight line. The Parkes NAR and the PPM employ different software techniques to counteract this characteristic, both of which are discussed in the next section. Additional methods of compensating for this and other front-end nonlinear behaviors are described elsewhere [8].

The RF detector assemblies (Fig. 3) provide two interfaces for controlling power measurement: an input selector switch and an RF attenuator. The input selector switch is a parallel TTL-controlled video switch used to select one of up to eight signal channels for measurement. The voltage-controlled attenuator is needed to adjust the signal level at the diode and set the desired baseline output frequency. Attenuation is minimized at -7 volts and increases exponentially as the control voltage approaches a limit of $+1$ volt.

The voltage-to-frequency units in the detectors were designed to output a frequency of 100 Hz with the detector switched to an internal ambient termination. The maximum output frequency that could be obtained with the Parkes unit was 13.7 kHz. As a result, the detector provided a dynamic range just exceeding the approximately 12.5 dB in input power experienced by the Parkes radiometer during operation. (System temperatures ranged from a zenith clear-weather value of 20 K to the antenna-ambient-termination-plus-noise-diodes value of 360 K.) This characteristic allowed the detector to be operated without changes in the internal attenuator setting, once the proper operating point was determined and the attenuator set accordingly. As discussed in the following section, this characteristic was crucial for maintaining a consistent calibration baseline.

3. Operation and Calibration. Although the Parkes radiometer is referred to as a noise-adding radiometer, the term is somewhat misleading: it could be operated as either a noise-adding radiometer (NAR) or as a total-power radiometer (TPR). In the TPR mode, the system temperature was derived from measurements of total RF power in the downconverter band. Therefore, system temperature was measured nonintrusively, but was subject to system gain instabilities and required periodic recalibration on the ambient load to maintain accuracy. In the NAR mode, system temperature was derived by Y-factoring power measurements made with the noise diodes modulating on and off. This mode reduced sensitivity to gain changes and provided better resolution when using larger noise diodes, but telemetry was degraded due to the noise injected into the system.

In the NAR mode, the operator could specify which noise diode to modulate by entering its temperature as a parameter. The FEC did not require an exact value; it would find the closest available diode and inform the operator of its choice. The FEC could also automatically monitor the system temperature and select a diode that would not increase the system noise temperature by more than two percent.

In the TPR mode, noise-power measurements were converted into system temperature using the fundamental relationship $P = GkTB$. The GkB value, referred to in FEC displays as the "system gain factor," varied with system gain and had to be calibrated prior to using the TPR, and periodically thereafter. The FEC performed a system gain factor calibration operation only for the maser channel selected. The automated sequence of events involved selecting the antenna ambient termination as the signal source for the receive chain, performing a power measurement with the RF detector, restoring the original configuration, and then solving for the system gain factor. Further system temperature calculations used this value until it was recalibrated at the request of the operator. Adding an optional numeric parameter to the command allowed manual setting of the system gain factor value.

Use of the NAR mode also required a calibration operation. Noise diode reference temperatures can only be measured in situ, and can vary in value as their environment changes, so they generally are measured prior to each use. The process of calibrating the entire noise diode set for the selected maser channel was automated using a calibration-transfer technique. This was done by selecting the antenna ambient load as the signal source, taking NAR Y-factor data using the largest noise diode, computing diode temperature from the data, selecting the feedhorn as the signal source, and measuring the sky temperature using the newly calibrated large diode. Once the sky temperature had been measured, each of the remaining diodes was selected for calibration using the sky temperature as a reference. Once all the diodes were calibrated, the original receive-chain signal source was restored. Adding an op-

tional numeric parameter to the command allowed manual setting of the temperature of the active noise diode.

An estimate of system linearity and NAR health could be obtained with a command measuring the additive noise temperature of a medium-power diode at two different system noise temperature levels and comparing the results. Typically, the radiometer first measured the baseline-feedhorn system temperature in the TPR mode and then the temperature with the medium diode turned on. Secondly, the TPR measured system temperature using the ambient load with the highest noise diode on and then with both the highest diode and the medium diode on. The differences between the two measurements at each operating point yielded a derived medium-diode temperature. The percent difference between the two derived values was reported to the operator as a measure of system linearity (Fig. 10).

Measurement resolution for a NAR is a function of integration time, diode temperature, system temperature, and noise bandwidth. For systems that are not gain-stable, NAR resolution is also affected by diode modulation rate. NARs are gain-insensitive only when individual measurement periods are short enough that the system gain does not change appreciably during sample integration. For short integrations, a pair of relative measurements eliminates the effects of a changing baseline power level. Slow diode modulation rates allow gain instability effects to appear and degrade resolution. High diode switching rates cause the controller to spend most of its time on processing overhead and very little time collecting data. In either case, measurement resolution decreases. A diode switching rate command provided the ability to adjust the diode modulation rate to obtain the best results (typically 10–15 Hz for Parkes and other DSN antenna systems).

In some cases, it was desirable to manually modulate the noise diodes or set the RF power-detector attenuator level. A manual command allowed the operators to force the diodes to turn on or off, or to return automatic control to the FEC. Another command allowed the operator to override the automatic adjustment of the internal attenuator and manually set an attenuation level.

An additional operating mode not normally accessed by the operator affected operation of the RF power detector. One of two methods of determining noise-power level with the detector could be selected. The default mode, referred to as the "linear" mode, used a second-order transfer function (based on original measurements of the equipment) to create a linearized relationship over the entire detector operating range. This relationship was between the RF power entering the assembly and the power reading computed by the driver routines. As a result, the location of the operating point was not critical; the internal attenuator was always automatically adjusted to center the range of measurable temperatures within the dynamic range of the detector, and then held constant until a change in system configuration was detected. This type of operation was critical for TPR mode use because of the large temperature difference between the ambient load calibration source and the feedhorn source. Without it, the internal attenuator would have to be adjusted to prevent clipping or to maintain a constant operating point, either of which would change calibration baselines and decrease accuracy.

The alternate RF detector operating mode, known as the "DSN" mode, was simpler and patterned after the method used by the DSN PPM NAR. This mode could only be used in conjunction with NAR operation, as it allowed the detector's internal attenuator setting to be altered, erasing any calibration baseline. The DSN mode dynamically fit a first-order equation to the detector frequency response, thereby restricting power measurements to a small, nearly linear region of the response curve. This was done by adjusting the internal attenuator to maintain a fixed output frequency for the diode off state prior to each measurement. Noise power was computed by dynamically fitting a first-order equation to the off measurement frequency and the detector's internal ambient termination rest frequency.

IV. Monitor and Control

Because the Parkes FEC was never required to be used at a Deep Space Communications Complex (DSCC), its command format and monitor displays were not required to follow DSN CMC/LMC interface agreements and convention. Originally, the FEC was to be connected to the PCTA; thus, to maintain compatibility, the FEC command structure and displays were designed to meet PCTA conventions. When the decision was made not to implement the PCTA controller link, the FEC became a standalone controller and was connected to the Canberra DSCC via a modem and data link.

V. Performance

A. Discussion

Probably the most important performance statistic for judging the quality of a radiometer is the degree to which it can resolve changes in system operating noise temperature. Reporting radiometer performance is not, however, as simple as quoting a measured value of temperature resolution.

Resolving capability depends on several factors: sample integration time, noise-diode temperature and switching rate (for NARs), the bandwidth of the detected signal, and the system temperature itself. As a result, radiometer performance is better expressed as temperature resolution versus integration time for a specified noise-diode temperature at a normalized system temperature.

In order to collect the data needed for radiometer performance analysis, it is necessary to fix some of the variables mentioned above. One of them, the system noise bandwidth, is usually fixed by the hardware. Another involves holding the operating temperature of the system constant during data taking, preferably at as low a temperature as possible. This is because resolution varies inversely with system temperature, and high system temperatures (such as those obtained when viewing the antenna ambient termination) can mask the performance capability of a sensitive radiometer. One solution is to switch the antenna front end to a cold load constructed from a waveguide termination immersed in a liquid nitrogen dewar. (Liquid helium would, of course, be even better.)

For convenience, DSN radiometer performance tests are usually conducted using a clear sky as a source with the antenna held steady, preferably at zenith to minimize the path length through the atmosphere. Under ideal atmospheric conditions, the sky at X-band appears as a constant source radiating at approximately 8.5 K. However, because the atmosphere contributes to the system operating temperature, and it is not constant, the system temperature does not stay constant. The most significant contributing factor at frequencies used by the DSN is water vapor. Unfortunately, even a sky that appears clear may still contain large, variable amounts of water vapor, making this technique only suitable for short test runs at best.

To obtain a thorough picture of radiometer performance under a wide variety of operating conditions, system temperature data need to be collected for several integration times and, in the case of NARs, using a variety of noise diodes. Calculating the standard deviation of each group of measurements yields resolution as a function of integration time and diode. Reducing all the data and plotting yields a family of curves that can be compared to theoretical curves.

Fortunately, the data collection process can be simplified. By operating the radiometer at the shortest integration time of interest and taking a large number of samples, it is possible to integrate groups of samples by hand to obtain data points corresponding to longer integration times. Data sets can be normalized to any desired system temperature, and performance with other noise diodes can be inferred from comparison to theoretical curves.

In interpreting a plot of radiometer performance curves, two things should be examined. The first, of course, is how closely the measured values compare to the corresponding theoretical curve. The second is not so obvious: the location of the theoretical curve itself. This curve is not a universal plot true of all radiometers; it is constructed for the characteristics of that particular radiometer and the conditions under which the data were gathered. It is entirely possible for a radiometer whose performance curve lies well above its theoretical curve to outperform a second system whose performance nearly equals theory.

B. Parkes NAR Performance Data

It is unfortunate that only minimal time was made available for system performance testing after the final version of the Parkes NAR was delivered and installed on the antenna. Immediately after encounter, the radiometer was disassembled and returned to JPL along with the rest of the X-band front-end equipment. As a result, inadequate performance data were obtained.

However, the Parkes NAR was designed to be used for spacecraft tracking as well as antenna-pointing calibration; consequently, the NAR was operated continuously while the station tracked Voyager 2 throughout encounter week to provide the Voyager radio science investigators with baseline system noise temperature data. Although this type of data is not ideally suited for radiometer performance measurements, a method was found to derive from it a single performance curve for the NAR. The development of this method and the final results are described next.

During the Voyager encounter tracks, the Parkes NAR was instructed to integrate samples for a period of one second using the 0.25-K noise diode. The antenna drive computer, already configured to digitize the NAR analog output to support antenna pointing calibration, was reprogrammed to receive the system temperature samples and record them to floppy disk throughout each track.

These data sets were recorded by the Parkes computer as raw analog-to-digital (A/D) converter values, not as operating system noise temperatures. Unfortunately, the proper conversion factors were not available to reconstruct the original system temperatures and the continuity of the data was disrupted by gaps due to tracking update activities. These factors necessitated additional steps in the data analysis, but did not impact the accuracy of the final

results. The conditions under which the data were taken were, however, significant: poor weather, a moving antenna, and the use of the smallest noise diode, which has the greatest variance in its calibrated value. These factors degraded the measured radiometer resolution, unfavorably biasing the final performance statistics.

C. Parkes Data Reduction

The first step toward reducing the encounter radiometric data was the transformation of the A/D values back to the original system temperature values. Fortunately, while the NAR was operating, the FEC was instructed to display a system temperature sample every 15 sec on the three control terminals. Because the "data link" terminal at the Canberra complex (an IBM PC) was programmed to log all terminal input/output in a large internal buffer, these system temperature values were captured, recorded on disk, and made available along with the A/D converter values.

This NAR log data set provided the information necessary for reconstructing the original noise temperature values computed by the Parkes NAR. (The data sets could not serve as a basis for NAR performance analysis because 14 out of every 15 samples had been lost; contiguous data were needed.)

Of the three A/D and four NAR log data sets returned to JPL on disk, only day-of-year (DOY) 238—the day following Neptune closest approach—existed electronically in both forms. It is this data set that forms the basis for the performance figures reported in this article.

Because each A/D data set was produced from a series of linear transformations (assuming linear responses from the associated hardware), the transformation back to system temperature values was also a linear process:

$$T_i' = mC_i + b \qquad (i = 1, 2, 3, 4, \ldots, n)$$

where

T_i' = transformed A/D converter sample i (best estimate of the original NAR T_i)

C_i = A/D converter sample i

m, b = transformation parameters

The transformation parameters were determined by modeling the A/D and NAR log data sets, then substituting the model parameters into the above equation and solving. Under more ideal measurement conditions, the models would be simply the means of the two data sets. However, because the antenna was in motion during the track, the varying length of the signal path through the atmosphere resulted in a constantly changing baseline system temperature. This required that a more complicated model be used.

In the simpler case, the system-temperature model consists of a constant term. Movement of the antenna introduces a second, time-varying component that accounts for the change in atmospheric signal path length. To simplify calculations, a plane-parallel model of the atmosphere was used; the relative increase in path length compared to zenith could then be expressed more simply as the secant of the zenith angle. Zenith angle can be easily computed for any time of day using the coordinates of the source, the antenna, and standard astronomical tables.

The resulting system temperature models are then

$$C_i = C_C + C_S \sec(\psi_i)$$

$$T_i = T_C + T_S \sec(\psi_i)$$

where

C_i, T_i = model values for each data set

C_C, T_C = model constant terms

C_S, T_S = model scaling factors for time-varying term

ψ_i = antenna zenith angle at time i

Model parameters were determined for each set using the least-squares method with the data values as the dependent variable and the corresponding $\sec(\psi_i)$'s as the independent variable.

Figure 11 depicts the NAR log data set for most of DOY 238 and its corresponding model curve. Imperfections in the fit indicate other physical processes (primarily weather) that could not be modeled, but do not significantly affect the transformation of the A/D data set. Once the models were constructed and the transformation parameters generated, the entire A/D data set for DOY 238 was converted to system temperature values. Because a necessary condition for reducing radiometric data to resolution figures is that the set have a constant mean, an additional manipulation was needed.

One method of normalizing the mean of the system temperatures would be to subtract the model value from

each data point and add a constant; however, this method is not sufficient. The problem is that sample resolution is a function of the system temperature, which not only requires that the mean be normalized, but that the variance be normalized as well.

The proper conversion equation can be determined by starting with the equation expressing ideal noise-adding radiometer resolution performance [5,6]:

$$\sigma_T = \frac{2T}{\sqrt{tB}}\left(1 + \frac{T}{T_D}\right)$$

where

σ_T = theoretical best resolution

T = system temperature during measurement, K

T_D = noise-diode temperature, K

t = sample integration time, sec

B = noise bandwidth as seen by RF power detector, Hz

A simplification can be made in this case, where $T \approx 25$ K and $T_D = 0.28$ K.

Then $T/T_D >> 1$ and the above equation simplifies to

$$\sigma_T = \frac{2T^2}{T_D\sqrt{tB}}$$

For samples taken with a constant integration time, this can also be expressed as

$$\frac{\sigma_T}{T^2} = \frac{2}{T_D\sqrt{tB}} = \text{constant}$$

This relationship provides the means for properly normalizing the mean and variance in the data set, provided an estimate of the true system temperature is known for every sample:

$$T_i'' = \frac{(T_i' - \mu_i)}{\mu_i^2} * {T_N}^2 + T_N$$

where

T_i'' = normalized system temperature sample i

T_i' = transformed A/D converter sample i

μ_i = mean or "true value" of T_i' (from model)

T_N = mean normalized system temperature

The mean at each point is estimated by modeling the data using the same method described earlier for converting the A/D data. Figure 12 shows a half-hour segment of A/D data that has been converted to its corresponding system temperature values and plotted, together with its modeled mean and then after normalization to a temperature of 20 K.

A total of 12 half-hour segments of data, each consisting of approximately 1700 one-second integrations, were analyzed for DOY 238. Once each segment had been normalized to a consistent mean and variance, it was reduced to seven resolution figures corresponding to integration times of 1, 2, 5, 10, 20, 50, and 100 seconds. Determining resolution for one-second integration times was straightforward, requiring only the calculation of the standard deviation of each block of points. Resolution for other integration times required additional manipulation of the data.

To obtain data for longer integration times, it was necessary to average together contiguous groups of one-second data points. This technique manually duplicates what the NAR does automatically when integrating for long periods. One consequence of doing so is that the resulting block of data is proportionally smaller than the original, which increases the variance in its calculated resolution.

Each of the half-hour data segments was expanded in this manner six times to produce a total of seven blocks of data. Next, the standard deviation of all seven blocks was calculated for each segment. The resulting twelve values associated with each integration time were then reduced statistically to generate the final performance results. These results, together with the theoretical curve, are tabulated in Table 2 and plotted in Fig. 13.

Although the Parkes NAR performance curve in Fig. 13 does not match the ideal peformance curve for a NAR with equivalent characteristics, it should not be expected to do so. The data from which this curve was derived were not well-suited for performance measurements, having been taken during cloudy weather while the antenna was in motion. These conditions will degrade measured resolution, biasing the performance figures. The actual performance of the Parkes NAR should lie somewhere between the measured and ideal curves.

VI. Summary

The Parkes front-end controller was designed as a cost-effective means of providing a DSN interface for support by the Parkes antenna during the Neptune encounter.

The FEC design maximized the use of existing front-end hardware, implemented in 1985 by ESA for the Uranus encounter, by adding special features and capabilities. In particular, a new noise-adding radiometer design was added that departed from standard DSN design.

Much of the design effort for the NAR focused on performance improvements and operational innovations necessitated by project requirements. The FEC/NAR performed without problems during the encounter and was removed from the Parkes antenna in October 1989.

Acknowledgments

The author would like to thank C. Stelzried for providing suggestions on NAR functionality and operation. Many thanks also to J. Loreman and D. Trowbridge for their support during development at JPL and to G. Baines and R. Jenkins for their support during on-site installation and testing. L. Hileman contributed a first draft coding of the FEC software.

References

[1] D. L. Trowbridge, J. R. Loreman, T. J. Brunzie, and B. Jenkins, "An 8.4-GHz Dual Maser Front End for Parkes Reimplementation," *TDA Progress Report 42-93*, vol. January–March 1988, Jet Propulsion Laboratory, Pasadena, California, pp. 214–228, May 15, 1988.

[2] D. L. Trowbridge, J. R. Loreman, T. J. Brunzie and R. Quinn, "An 8.4-GHz Dual-Maser Front-End System for Parkes Reimplementation," *TDA Progress Report 42-100*, vol. October–December 1989, Jet Propulsion Laboratory, Pasadena, California, pp. 301–319, February 15, 1990.

[3] L. Fowler and M. Britcliffe, "Traveling-Wave Maser Closed Cycle Refrigerator Data Acquisition and Display System," *TDA Progress Report 42-91*, vol. July–September 1987, Jet Propulsion Laboratory, Pasadena, California, pp. 304–311, November 15, 1987.

[4] C. D. Bartok, "Analysis of DSN PPM Support During Voyager 2 Saturn Encounter," *TDA Progress Report 42-68*, vol. October–December 1981, Jet Propulsion Laboratory, Pasadena, California, pp. 139–150, February 15, 1982.

[5] P. D. Batelaan, R. M. Goldstein, and C. T. Stelzried, "A Noise-Adding Radiometer for Use in the DSN," *JPL Space Programs Summary 37-65*, vol. 2, Jet Propulsion Laboratory, Pasadena, California, pp. 66–69, September 30, 1970.

[6] T. J. Brunzie, "A Noise-Adding Radiometer for the Parkes Antenna," *TDA Progress Report 42-92*, vol. October–December 1987, Jet Propulsion Laboratory, Pasadena, California, pp. 117–122, February 15, 1988.

[7] M. S. Reid, R. A. Gardner, and C. T. Stelzried, "The Development of a New Broadband Square Law Detector," *JPL Technical Report 32-1526*, vol. XVI, Jet Propulsion Laboratory, Pasadena, California, pp. 78–86, August 15, 1973.

[8] C. T. Stelzried, "Non-Linearity in Measurement Systems: Evaluation Method and Application to Microwave Radiometers," *TDA Progress Report 42-91*, vol. July–September 1987, Jet Propulsion Laboratory, Pasadena, California, pp. 57–66, November 15, 1987.

Table 1. Parkes radiometer specifications

Parameter	Specification
General	
Number of receiver channels supported	Two, switchable
Signal sources (per receive channel)	Antenna feedhorn; aerial cabin ambient termination
Radiometer operating modes	Total power; noise-adding
Nominal system noise temperature range	15 to 400 K
RF detector	
Detector dynamic range	13.5 dB
Nominal input noise power level	−45 dBm
Input frequency bandwidth	65 MHz
Internal attenuator control	Manual or automatic
Internal attenuator range	0 to 50 dB
Detector operating modes	Dynamic first-order fit over subrange of detector response; static second-order fit over entire range of detector response
Noise diodes	
Diode selection control	Manual or automatic
Automatic diode selection criteria	<0.1 dB added noise
Nominal diode temperatures	0.25,0.5,1,2,4,8,50,(50+8) K
Diode modulation control	Manual or automatic
User-specifiable modulation frequency range	0.01 to 100 Hz
Sampling	
Sampling criteria	Integration time; sample resolution
User-specifiable sample integration time range	0.01 to 100 seconds
User-specifiable sample resolution range	0.001 to 10 K/sample
Sample output	
Measurement modes	Manual single-sample; continuous in background
Sample output modes	Display and analog output; analog output only
User-specifiable sample display interval	1 to 15 seconds/sample
Samples used in resolution calculation	None or 2 to 100
Analog output	
Ouput voltage range	−5 to +5 volts
Output resolution	2.4 mV (12-bits)
User-specifiable zero-volt noise temperature	0 to 500 K
User-specifiable noise temperature/voltage ratio	0.001 to 100 K/V
Calibration	
Total power radiometer mode	System gain factor
Noise-adding radiometer mode	Noise-diode temperatures
Linearity measurement points	Feedhorn/feedhorn+50 K; ambient/ambient+50 K; feedhorn/ambient+50 K

Table 2. Detail of Parkes noise-adding radiometer resolution performance summary

Data block	Sample integration time						
	1 sec	2 sec	5 sec	10 sec	20 sec	50 sec	100 sec
1	0.384	0.312	0.215	0.162	0.127	0.088	0.060
2	0.351	0.280	0.188	0.140	0.098	0.058	0.042
3	0.377	0.308	0.211	0.156	0.127	0.088	0.067
4	0.459	0.352	0.268	0.189	0.140	0.097	0.076
5	0.389	0.314	0.223	0.166	0.119	0.076	0.046
6	0.374	0.303	0.207	0.156	0.122	0.079	0.057
7	0.367	0.292	0.192	0.140	0.094	0.058	0.042
8	0.384	0.307	0.216	0.158	0.111	0.077	0.050
9	0.385	0.310	0.208	0.153	0.118	0.058	0.038
10	0.376	0.298	0.212	0.139	0.097	0.063	0.042
11	0.372	0.306	0.200	0.146	0.102	0.066	0.037
12	0.366	0.295	0.201	0.142	0.101	0.063	0.046
Total no. data points	20241	10118	4043	2019	1008	399	196
Average resolution, K	0.382	0.306	0.212	0.154	0.113	0.073	0.050
Standard deviation of resolution	0.02	0.01	0.02	0.01	0.01	0.01	0.01
Ideal performance, K	0.355	0.251	0.159	0.112	0.079	0.050	0.036

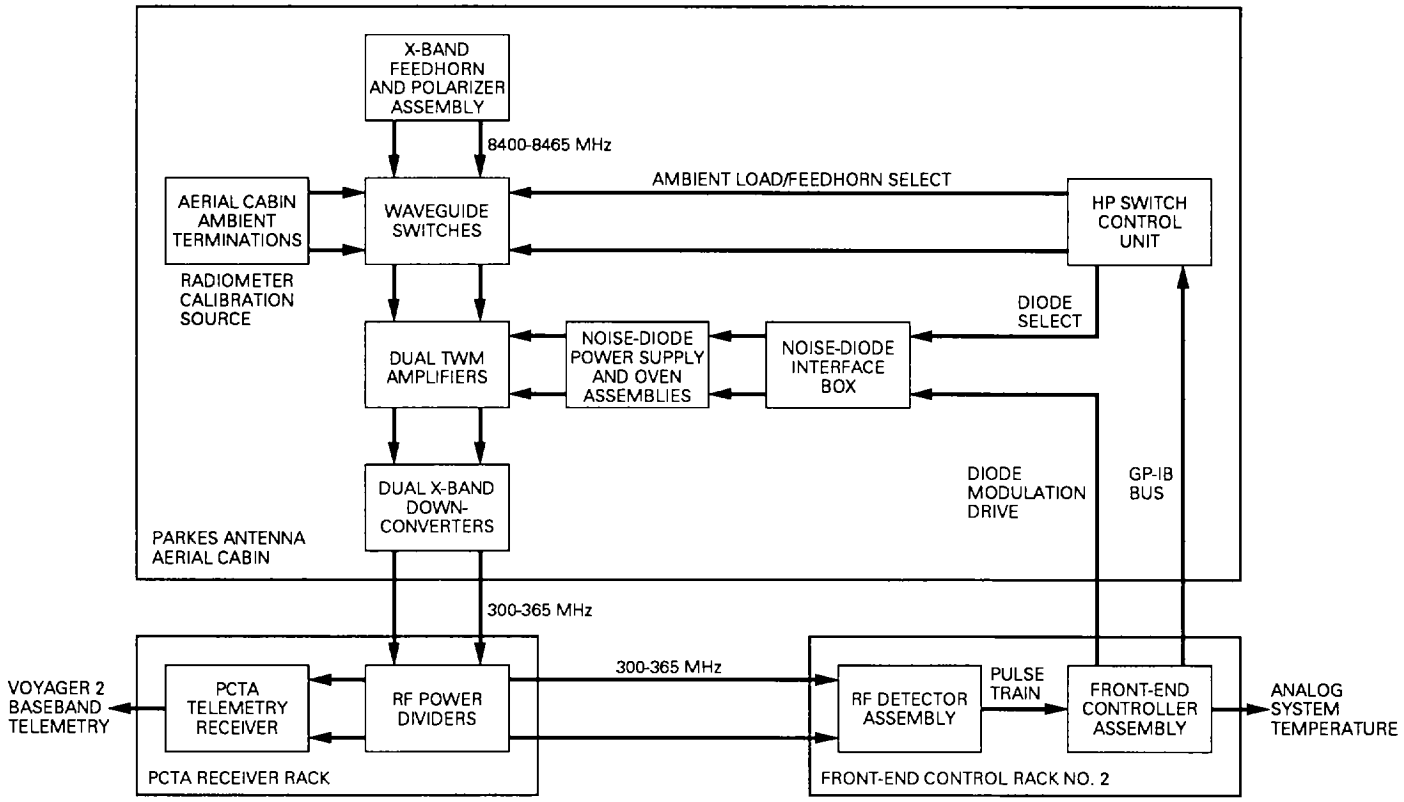

Fig. 1. Parkes front end (radiometer emphasized).

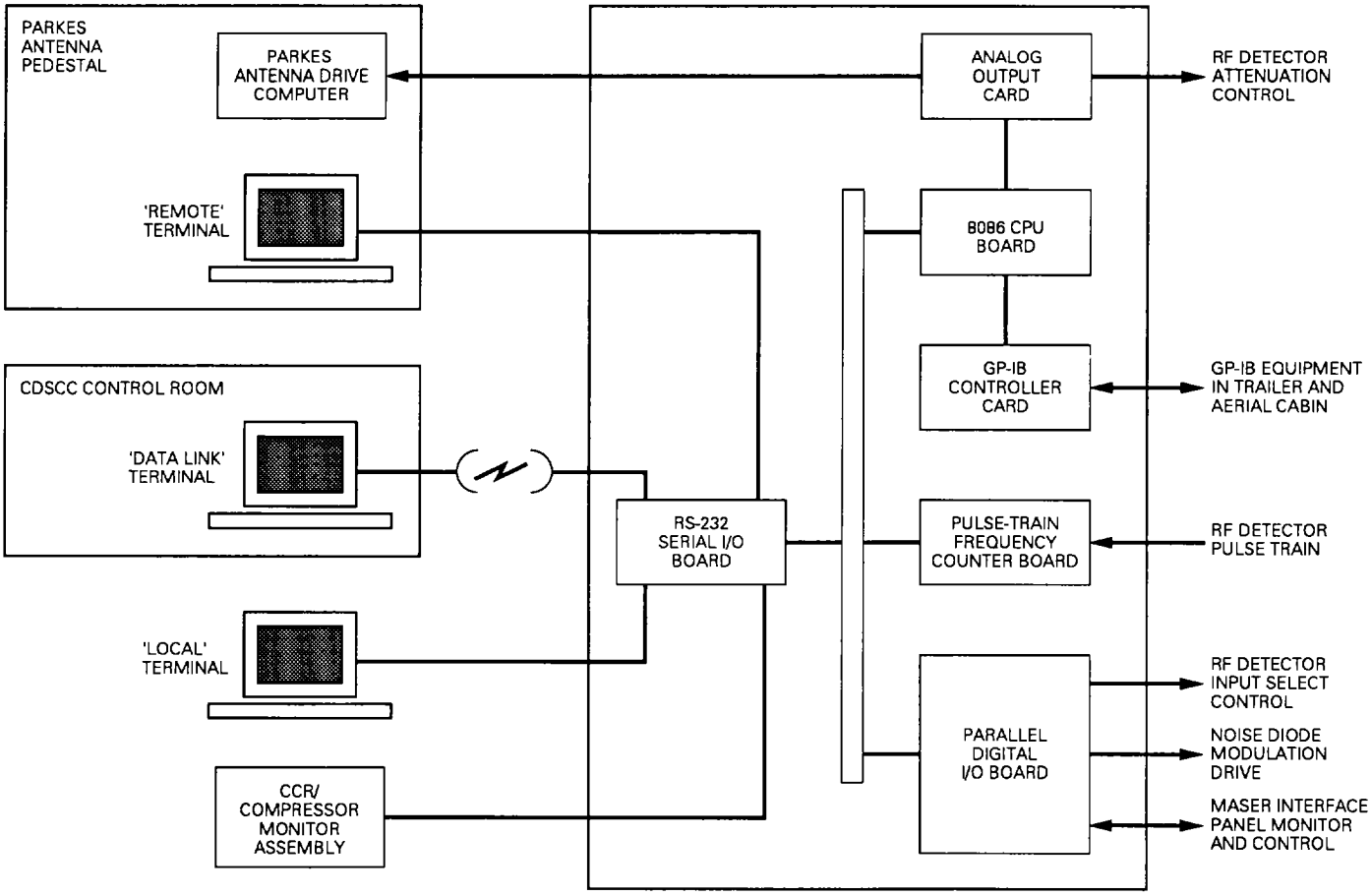

Fig. 2. Parkes front-end controller assembly.

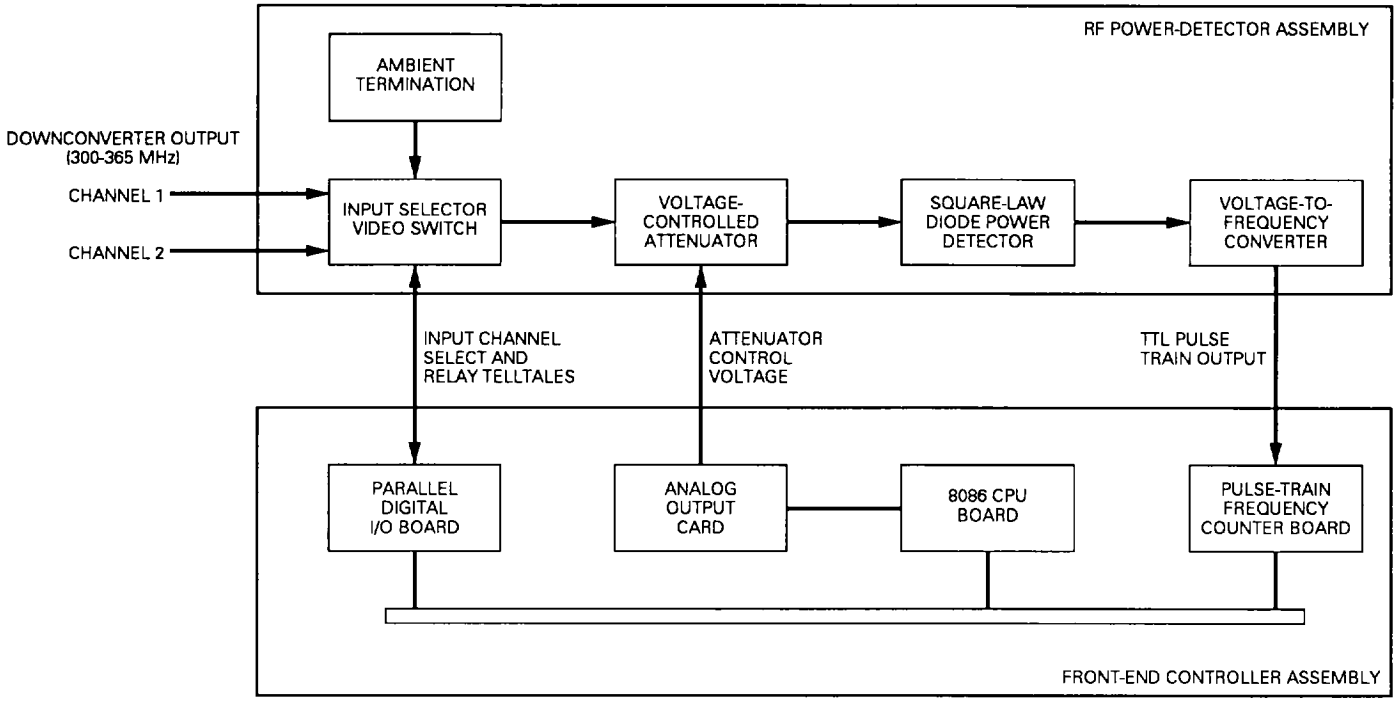

Fig. 3. Parkes radiometer RF power detector.

```
PFEC>help m

PFEC Front End Controller Measurement Help...
The format for user input is: COMMAND PARAMETER

  Cmnd  Description                          Parameter

  YFAC  Perform Y-factor Measurement.        [1],[2] [L]eft,[R]ight
  GAIN  Compute Maser Gain Profile.          [1],[2]
  PMTR  Operate Power Meter.                 [M]easure,[C]alibrate
  CCRH  Chart CCR Performance History.       [1],[2] [MMddHHmm] [MMddHHmm]
  SYST  Measure System Temperature (NAR).    [],[OFF],[C]ont,[D]isp [n] sec
  NRES  Set NAR Sample Resolution.           [n] Kelvins
  NRAT  Set NAR Sample Rate.                 [n] Hz
  DRAT  Set NAR Diode Switching Rate.        [n] Hz            (Debug only)
  NSAM  Set Number of Resolution Samples.    [n]
  CALG  Calibrate System Gain Factor.        [],[n] nW/Kelvin    (CFG only)
  CALD  Calibrate Noise Diodes.              [ALL],[n] Kelvins   (CFG only)
  DLTA  Measure System Linearity Delta.      [S]ky,[A]mbient,[F]ull Range

PFEC>
```

Fig. 4. Parkes FEC/NAR measurement help menu.

```
PFEC>help n

PFEC Front End Controller NAR Help...
The format for user input is: COMMAND PARAMETER

  Cmnd  Description                              Parameter

  PNAR  Set Parkes NAR Command Mode.             [OFF],[CFG],[OPR]
  NRCV  Set NAR Input Source.                    [1],[2],[TRM]
  NMOD  Set Total Power or Noise-Adding Mode.    [TPR],[NAR]
  DMOD  Set Square-Law Detector Operating Mode.  [LIN],[DSN]            (Debug)
  DIOD  Set NAR Diode Temperature.               [A]uto,[OFF],[n] Kelvins (NAR)
  DACZ  Set NAR D/A Zero-Volt Temperature.       [A]uto,[n] Kelvins
  DACG  Set NAR D/A Temperature Gain.            [A]uto,[n] Kelvins/Volt
  NOIS  Turn Noise Diodes On or Off.             [A]uto,[OFF],[ON]      (Debug)
  NATN  Set RF Assy Internal Attenuator.         [A]uto,[n] Volts       (Debug)
  TMAS  Set Maser Input Noise Temperature.       [1],[2] [n] Kelvins
  TFOL  Set System Follow-up Noise Temperature.  [1],[2],[M]onRcvr [n] Kelvins
  GINS  Set Maser Gain Instability.              [S]hort-term [n] dB,
                                                    [L]ong-term [n] dB/hr

PFEC>
```

Fig. 5. Radiometer configuration help menu.

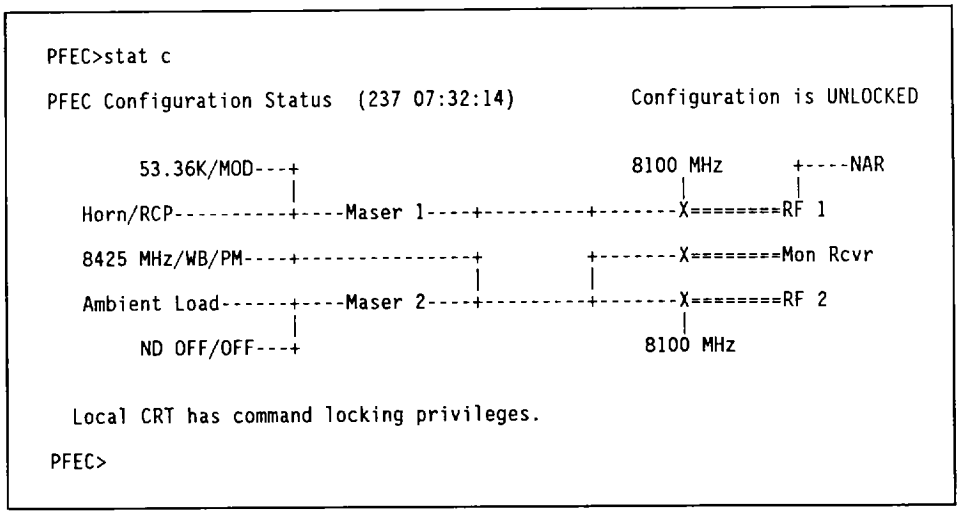

Fig. 6. Front-end configuration status display.

```
PFEC>stat m

PFEC Temperature Measurement Status  (236 13:27:54)

                                    RF Ch 1       RF Ch 2

  System Temperature          :      15.328        15.037      Kelvins
  Measurement Resolution      :       0.025         0.021      Kelvins

  Ambient Load Temperature    :     297.860       300.163      Kelvins

  System Gain Factor          :      12.823         8.983      nW/Kelvin
  Gain Factor Age             :    00:02:38      00:13:25

  Maser Input Noise Temp      :       4.05          3.92      Kelvins
  System Follow-up Noise Temp :       0.13          0.29      Kelvins

  Short-Term Gain Instability :       0.03          0.03      dB
  Long- Term Gain Instability :       0.10          0.10      dB/hr

  TPR Resolution Uncertainty  :      0.013         0.283      Kelvins

PFEC>
```

Fig. 7. Radiometer temperature measurement status display.

```
PFEC>stat n

PFEC Radiometer Status  (238 11:55:08)

  Parkes NAR Command Mode         :  Configuration
  Radiometer Operating Status     :  Running on Channel 2
  Radiometer Operating Mode       :  Total Power
  RF Assembly Detector Mode       :  Linear Response

  Integration Time Criteria       :  Sampling Rate
  Measurement Sample Time         :  10.0 Hz
  Measurement Resolution          :   0.030 Kelvins

  D/A Maximum Output Temperature  :  27.50  Kelvins
  D/A Zero-Volt Temperature/Gain  :  25.00  Kelvins  /  0.500 Kelvins/Volt
  D/A Minimum Output Temperature  :  22.50  Kelvins

  Noise Diode Selection           :  51.263 Kelvins, Manually
  Noise Diode Modulation          :  Automatically Controlled
  RF Assembly Internal Attenuator :  -3.832 Volts, Auto-Adjusted

PFEC>
```

Fig. 8. Radiometer configuration status display.

```
PFEC>stat d

PFEC Noise Diode Status  (241  12:17:31)

                                    RF Ch 1       RF Ch 2

  Noise Diode Temperatures    :       0.223         0.250       Kelvins
                              :       0.483         0.500       Kelvins
                              :       1.183         1.000       Kelvins
                              :       2.089         2.000       Kelvins
                              :       3.938         4.000       Kelvins
                              :       9.032         8.000       Kelvins
                              :      52.382        50.000       Kelvins
                              :      61.414        58.000       Kelvins

  Noise Diode Calibration     :   Calibrated    Not Cal'd

PFEC>
```

Fig. 9. Noise diode status display.

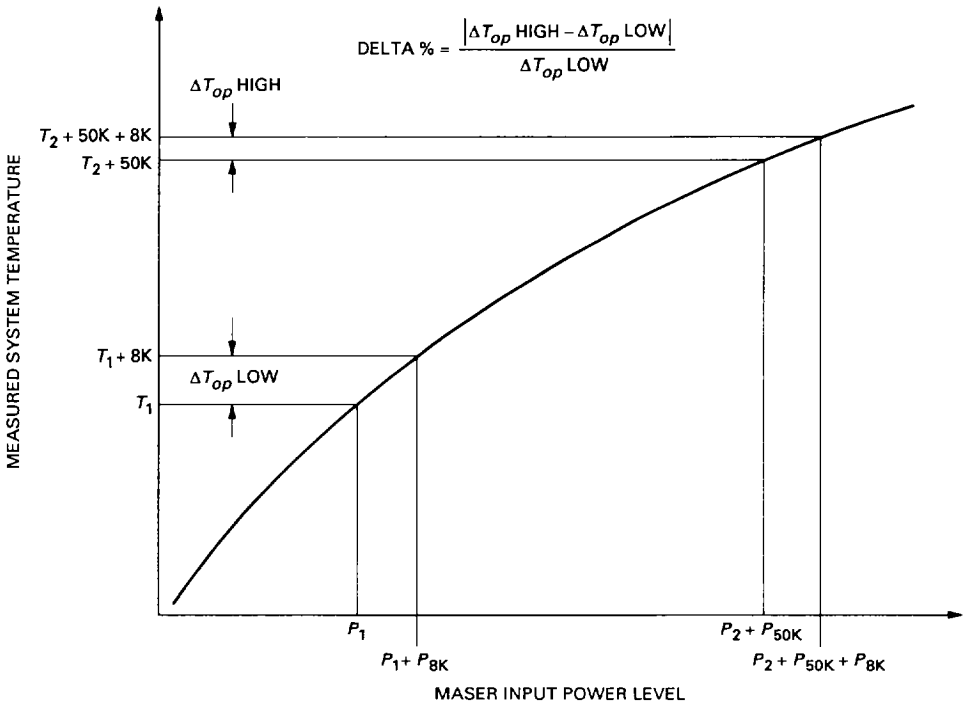

Fig. 10. Parkes radiometer "Delta" command.

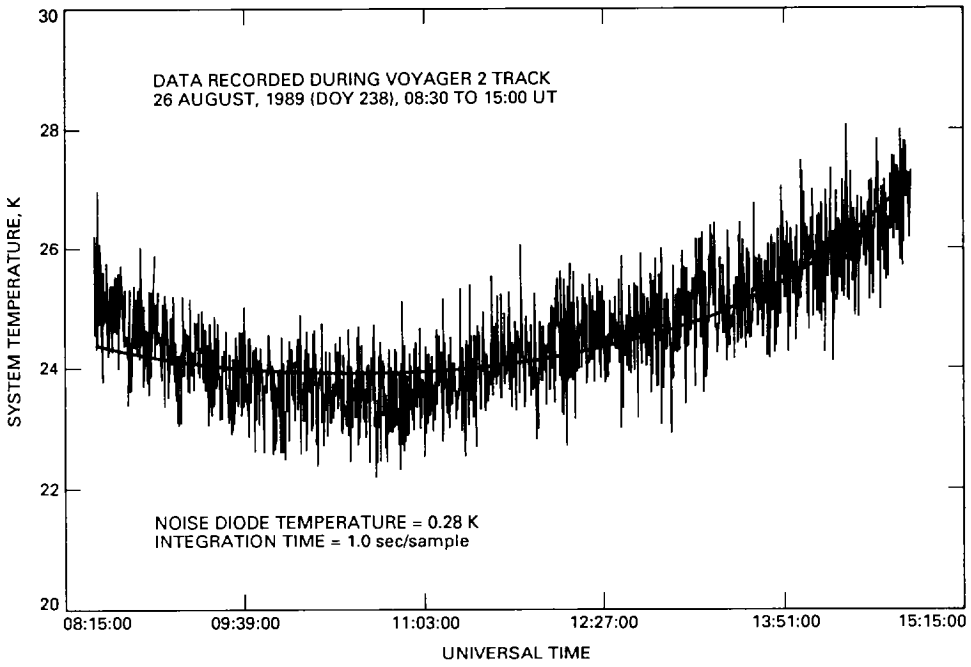

Fig. 11. Logged NAR data and corresponding system noise temperature model.

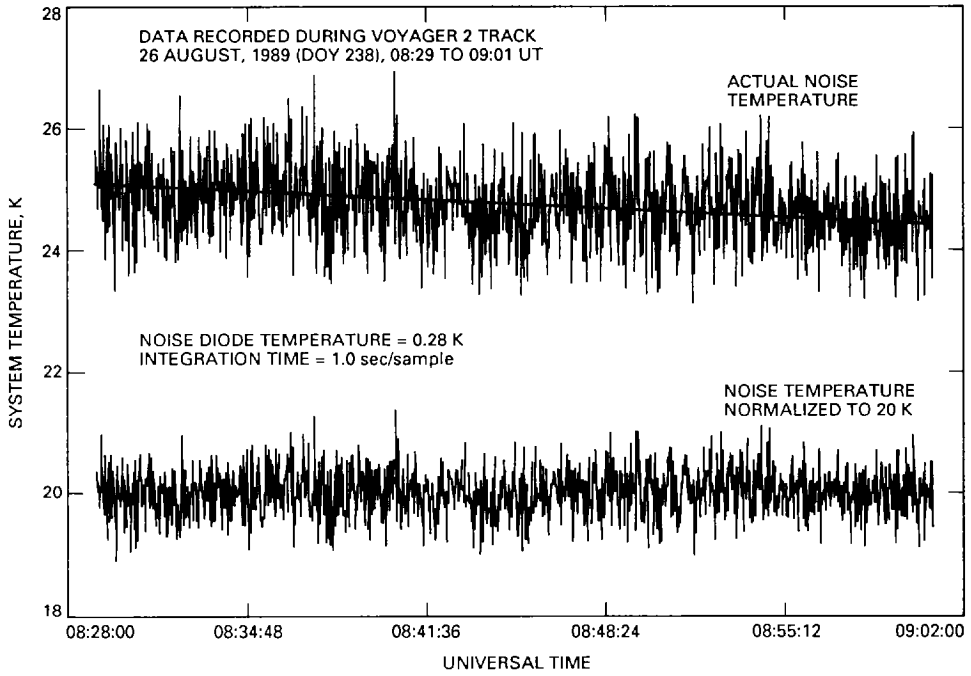

Fig. 12. Transformed A/D data, model, and normalized system noise temperatures.

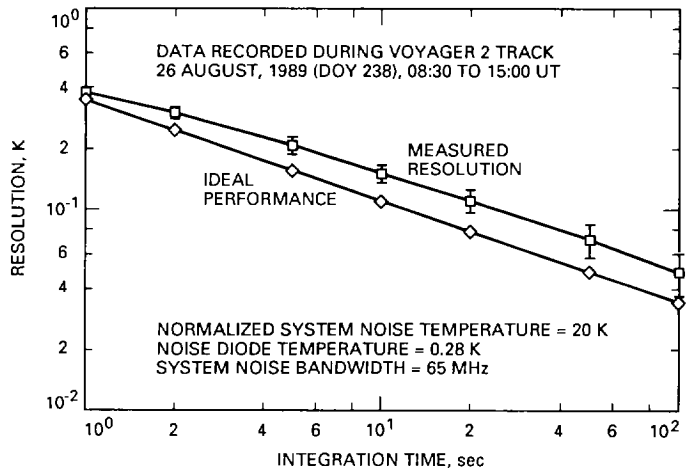

Fig. 13. Parkes noise-adding radiometer resolution performance summary.